Improvement of the behaviour of composite slabs: A new type of end anchorage

Alexandre Fonseca [a], Bruno Marques [b] and Rui Simões [*c]

ISISE, Civil Engineering Department, University of Coimbra, Coimbra, Portugal

Abstract. The application of composite steel-concrete slabs with profiled steel sheeting has increased, due to the various advantages in relation to reinforced concrete slabs such as, the reduced thickness, the reduced amount of lost formwork needed, as well as the speed of execution. The loss of longitudinal shear resistance is, generally, the governing design mode for simply supported spans of common lengths. For common distributed loadings, the composite behaviour is influenced by the partial shear connection between the concrete and the steel sheeting. The present research work is intended to contribute to improving the ultimate limit state behaviour of composite slabs using end anchorage. Eurocode 4, Part 1.1 (EN 1994-1-1) provides an analytical methodology for predicting the increase of longitudinal resistance, achieved by using shear studs welded through the steel sheeting as the end anchorage mechanism. The code does not supply an analytical methodology for other kinds of end anchorage so, additional tests or studies are needed to prove the effectiveness of these types of anchorage. The influence of end anchorage mechanisms provided by transverse rebars at the ends of simply supported composite slabs is analysed in this paper. Two experimental programmes were carried out, the first to determine the resistance provided by the new end anchorage mechanism and the second to analyse its influence on the behaviour of simply supported composite slabs.

1. Introduction

A composite steel-concrete slab is a type of slab where cold-formed steel sheeting acts as a loss formwork supporting the weight of wet concrete as well as the construction loads. After the curing of the concrete, the two materials combine to form a composite member where the profiled steel sheeting constitutes a part or the totality of the tension reinforcement.

This type of slab is widely used in the floor systems of steel buildings; it is an efficient structural system since the steel sheeting supports all the construction loads during the construction stage, without any, or with just a reduced number of, props (Johnson 2004). The design of a composite slab may be governed by one of the following three collapse modes: vertical

---

*Corresponding author, Assistant Professor, E-mail: rads@dec.uc.pt
[a] Master Student
[b] Civil Engineerr

shear, longitudinal shear, bending moment, or, additionally, by serviceability conditions. In general, the main collapse mode is longitudinal shear (Lopes and Simões 2008), for load levels significantly lower than those necessary to reach the other collapse modes mentioned. Therefore, if the longitudinal shear resistance of a composite slab is improved, its load capacity will be increased.

In Europe, the design of composite slabs is regulated by EN 1994-1-1 (CEN 2007), which states that the longitudinal shear resistance is achieved by the mechanical interlock provided by small deformations of the sheet (embossments and indentations) or the frictional interlock in profiles shaped in a re-entrant form. This resistance may be increased by developing end anchorage mechanisms. In EN 1994-1-1 (CEN 2007) two end anchorage mechanisms are predicted (Fig. 1): (i) welded studs or other types of local connection between the concrete and the steel sheeting, in combination with mechanical or frictional interlock; and (ii) deformation of the ribs at the end of the steel sheeting, only in combination with frictional interlock (re-entrant profiles). Using welded studs as the end anchorage mechanism can only be achieved if the studs are welded to the beam flange through the steel sheeting, which implies that the studs must be welded on site. The methods most used in the various design codes for the longitudinal shear design of composite slabs (such as EN 1994-1-1) are: (i) the *m-k* method; and (ii) the partial connection method. The *m-k* method is, in general, more conservative and it does not allow the inclusion of end anchorage mechanisms or additional longitudinal bottom reinforcement without additional tests to include these additional variables (Johnson and Anderson 2004). The partial connection method has its basis on a graph that relates the bending moment along the slab with the degree of shear connection. The method is only applicable to ductile slabs but it has the advantage of being able to include end anchorage mechanisms or longitudinal bottom reinforcements, without the need of additional tests (Johnson and Anderson 2004).

For a number of years some researchers have tried to improve the longitudinal shear resistance of composite slabs; therefore, a brief review of some papers concerning this subject will be

(a) Shear studs   (b) End deformation
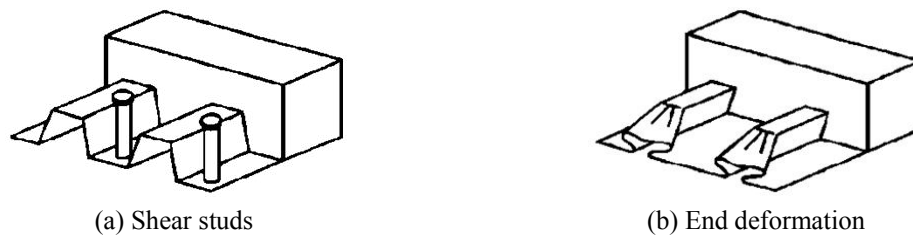
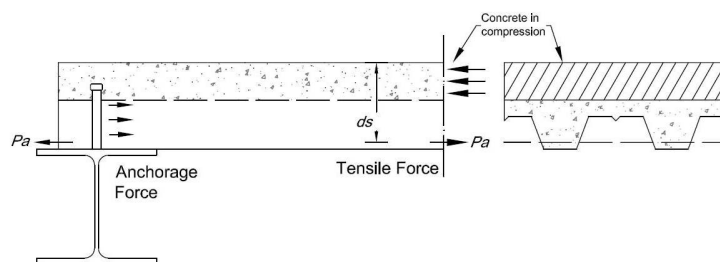Fig. 1 End anchorage mechanisms of EN 1994-1-1

Fig. 2 Behaviour of end anchorage in composite slabs (adapted from Jolly and Lawson (1992))

presented in the following paragraphs.

In 1992, C. Jolly and R. Lawson performed an experimental study to analyse the influence of end anchorage mechanisms on the load capacity of composite slabs (Fig. 2). Their experimental programme consisted of testing composite slabs with and without end anchorage. By comparing these experimental results, they concluded that the former had almost twice the resistance of the latter. It was also noted that the stiffness of the end anchorage mechanism is lower than the stiffness of the mechanical interlock provided by the embossments on the steel sheeting in the study; consequently, the authors proposed that only half of the resistance of the end anchorage mechanism should be taken into account (Jolly and Lawson 1992).

In 2003, S. Chen published a paper where he experimentally compared the behaviour of composite slabs without end anchorage with slabs with end anchorage using stud bolts (Chen 2003). From his research, he concluded that the collapse of slabs without end anchorage was brittle because after the initial slip the load decrease was quick and flexural cracks appeared in the concrete. Moreover, slabs with end anchorage had an almost linear load-deflection curve before initiation of shear-bond slip. By comparison of his experimental results with a prediction obtained using Jolly and Lawson's proposal (Jolly and Lawson 1992), he concluded that the reduction factor for the end anchorage should be 0.3 instead of 0.5, since the latter leads to unsafe predictions.

M. Ferrer tried to improve the longitudinal shear resistance of a composite slab, just by improving the geometry of the profiled steel sheeting (Ferrer *et al*. 2005). By means of experimental and numerical analysis they showed that changing some parameters, like the depth of the embossments or their orientation, it is possible to achieve an enhanced connection between the steel and concrete.

Fig. 3 displays the approach taken by Chuan *et al*. (2008) for improving the longitudinal shear resistance; it consists in the application of shear screws at the interface of the steel sheeting and the concrete. By comparing the experimental results of slabs with and without screws they concluded that the slabs with screws make it possible to reach a higher resistance and deformation capacity.

In the University of Coimbra, Carmona *et al*. (2009) studied the effect of the placement of transversal rebars along the slabs, crossing the ribs perpendicularly. With this improvement in the slabs, higher longitudinal shear resistance and less up-lift effect were achieved.

In June 2011, Chen *et al*. presented a detailed study concerning the shear bond failure of composite slabs (Chen *et al*. 2011). The longitudinal shear forces of thirteen specimens, varying the span length, the slab depth, the shear span length and the end anchorage provided by steel headed studs, were deduced from experimental results. A new improved method for determining the bending moment resistance of a composite slab, based on the partial shear connection at the ultimate limit state, was defined and validated. This method includes the addition of two reduction

Fig. 3 Steel deck with screws drilled from the bottom side (left) and a view from the top side (right)

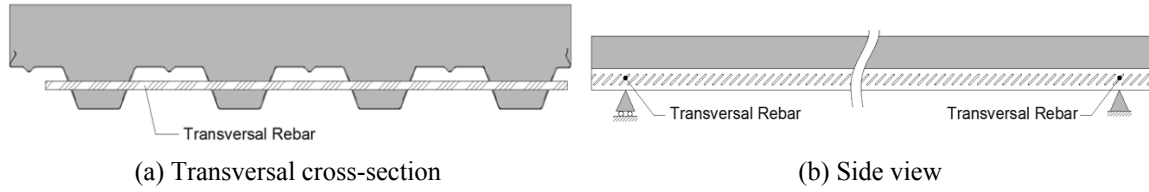(a) Transversal cross-section   (b) Side view

Fig. 4 Alternative end anchorage mechanism

coefficients to the partial shear connection method predicted in EN 1994-1-1 (CEN 2007).

The alternative end anchorage mechanism presented in this paper consists of inserting transversal rebars across pre-drilled holes in the steel sheeting web, close to the slab supports (Fig. 4). The effectiveness of this mechanism is independent of the type and material of the supporting beams; if the supporting beam is a steel section, studs can be used just to achieve composite beam action, thus avoiding welding the studs through the steel sheeting on site. The study of this end anchorage mechanism was divided in two parts: the first consisted of an experimental study regarding the resistance of the end anchorage mechanism (Section 3) and the second consisted of an experimental study performed to obtain the resistance of composite slabs using this type of end anchorage (Section 4). The objective of the first part of the study was to determine the characteristic resistance of the end anchorage mechanism, using the statistical analysis presented in Annex D of EN 1990 (CEN 2002a). In the second part, the bending resistance of several slabs was determined experimentally and compared with the prediction obtained by the partial connection method of EN 1994-1-1 (CEN 2007).

2. Partial connection method with end anchorage

2.1 Design procedure with end anchorage

The partial connection method may be reformulated in a way to include the end anchorage force (CEN 2007). For this purpose, the compression force in the concrete slab N_c (see Fig. 5) shall be increased with the value of the design resistant force F_{ea} (Eq. (1)) of the end anchorage. So, the compression force in the concrete slab N_c (not higher than the equivalent force N_{cf}, in the case of full shear connection) in a cross-section, at a distance L_x from the nearest support, is given by

$$N_c = \tau_{u,Rd}\ b\ L_x + F_{ea} \leq N_{cf},$$ (1)

where:

$\tau_{u,Rd}$	is the design shear strength at the steel-concrete interface,
b	is the width of the slab under analysis (in general, the width of one rib),
L_x	is the distance from a cross-section to the nearest support.

The end anchorage resistant force F_{ea} may be the force $P_{pb,Rd}$ defined in EN 1994-1-1 (CEN 2007) for the end anchorage achieved by headed studs welded through the steel sheet; in the scope of the present work, taking into account the end anchorage mechanism considered, this force is given by the lower value between the bearing resistance of the steel sheet $F_{b,Rd}$ or the shear resistance of the transversal rebars, as will be described in Section 3 of the present paper.
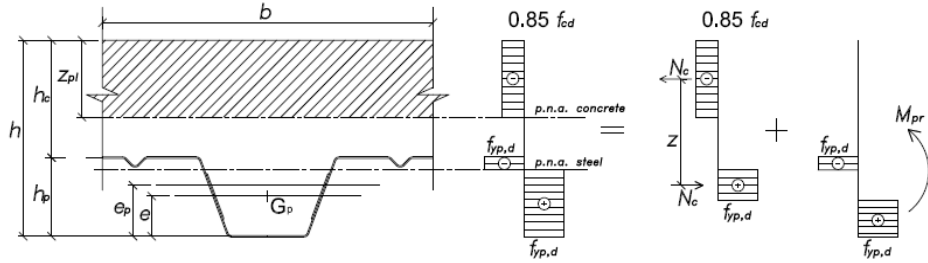
Fig. 5 Plastic stress distribution for sagging bending moment if the neutral axis is within the steel sheeting

In Eq. (1) the design shear strength $\tau_{u,Rd}$ is determined through the tests on composite slab models without any reinforcement as prescribed in EN 1994-1-1 (CEN 2007). The remaining formulation of the partial connection method is described below. The resistant bending moment M_{Rd} at a distance L_x from the nearest support is given by Eq. (2) in accordance with Fig. 5.

$$M_{Rd} = N_c\, z + M_{pr}, \tag{2}$$

$$M_{pr} = 1.25 M_{pa}\left(1 - \frac{N_c}{N_{pa}}\right) \le M_{pa}, \tag{3}$$

$$z = h - \frac{z_{pl}}{2} - e_p + (e_p - e)\frac{N_c}{N_{pa}}, \tag{4}$$

$$z_{pl} = \frac{N_c}{0.85\, f_{cd}\, b} \le h_c, \tag{5}$$

$$N_{pa} = A_{pe}\, f_{yp,d}, \tag{6}$$

where:
  M_{pa} is the design value of the plastic resistant bending moment of the effective cross-section of the profiled steel sheeting,
  A_{pe} is the effective cross-sectional area of the profiled steel sheeting,
  $f_{yp,d}$ is the design value of the yield strength of the profiled steel sheeting, given by f_{yp}/γ_M, where f_{yp} is the characteristic value of the yield strength and $\gamma_M = 1.00$ the safety factor,
  f_{cd} is the design value of the cylinder compressive strength of concrete, given by f_{ck}/γ_C, where f_{ck} is the characteristic value of the compressive strength and $\gamma_C = 1.50$ the safety factor,
  e is the centroidal axis of the profiled steel sheeting,
  e_p is the plastic neutral axis of the profiled steel sheeting.

The remaining symbols are defined in Fig. 5.

2.2 Design procedure with end anchorage and longitudinal reinforcement rebars

To predict the resistant bending moment M_{Rd} through the partial connection method (Eq. (7)), including the force N_{as} due to the longitudinal reinforcement rebars (with cross section area A_s in
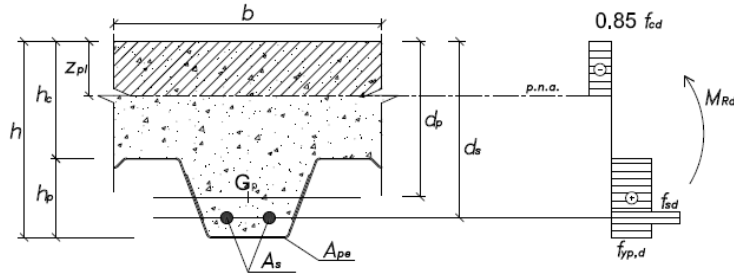
Fig. 6 Plastic stress distribution for sagging bending moment on a section with reinforcement rebars

the width *b*), the method prescribed in prENV 1994-1-1 (CEN 1992) is used, as described by the following

$$M_{Rd} = N_c z_1 + M_{pr} + N_{as} z_2,$$ (7)

$$N_c = b\, L_x\, \tau_{u,Rd} + F_{ea},$$ (8)

$$N_{as} = A_s\, f_{sd},$$ (9)

$$z_2 = d_s - 0.5 z_{pl},$$ (10)

$$z_1 = h - 0.5 z_{pl} - e_p + (e_p - e)\frac{N_c}{N_{pa}},$$ (11)

$$z_{pl} = \frac{N_c + N_{as}}{0.85\, f_{cd}\, b} \le h_c,$$ (12)

where: f_{sd} is the design value of the yield strength of the longitudinal rebars given by f_{sk}/γ_s, where f_{sk} is the characteristic tensile strength and $\gamma_s = 1.15$ is the partial safety factor. Other symbols are represented in Fig. 6 or given in Section 2.1.

3. End anchorage mechanism with transversal rebars

3.1 Design models

The shear resistance of the rebar or the bearing resistance of the steel sheeting, may govern the resistance provided by the end anchorage mechanism studied in this work. The shear resistance of the rebar $F_{v,Rd}$ can be estimated by Eq. (13) (by analogy with the shear resistance of a bolt) which is presented in EN 1993-1-8 (CEN 2010).

$$F_{v,Rd} = \frac{\alpha_v\, f_{ub}\, A}{\gamma_{M2}},$$ (13)

where:
   A is the area of the cross-section of the rebar,

f_{ub} is the ultimate strength of the steel of the rebar,
α_v is a parameter dependent of the steel grade;
γ_{M2} is the partial safety factor (with a recommended value equal to 1.0).

The bearing resistance of the steel sheeting may be estimated by the Eq. (14), in accordance with EN 1993-1-3 (CEN 2004).

$$F_{b,Rd} = \frac{2.5\,\alpha_b\,k_t\,f_u\,d\,t}{\gamma_{M2}},$$ (14)

where:

$\alpha_b = \min\{1.0;\, e_1/(3d)\}$,
$k_t = (0.8t + 1.5)/2.5$, if 0.75 mm $\leq t \leq 1.25$ mm and $k_t = 1.0$ if $t > 1.25$ mm,
e_1 is the distance to the end of the steel sheeting,
d is the rebar diameter,
t is the thickness of the steel sheeting,
f_u is the ultimate strength of the steel sheeting.

For typical grades and geometries of steel sheeting (thicknesses between 0.8 and 1.2 mm) and rebars (above 8 mm diameter), the bearing resistance of the steel sheeting (Eq. (14)) is generally the governing collapse mode. The use of Eq. (14) for estimating the bearing resistance of the steel sheeting may lead to an overestimation, since this expression was derived for clamped sheets, as in bolted joints; therefore, this expression must be calibrated beforehand, in order to determine the correct resistance of the proposed end anchorage mechanism, which is presented in the following section.

3.2 Statistical analysis of EN 1990 Annex D

As mentioned before, the objective of the first experimental study was to determine the characteristic values for the end anchorage resistance; as well as to calibrate an analytical resistance model based on that prescribed in EN 1993-1-3 (CEN 2004), applicable to clamped sheets. To achieve this objective, the experimental results were analysed in accordance with the statistic methodology presented in Annex D of EN 1990 (CEN 2002a), which is directed at design assisted by tests; the determination of the characteristic values of a property is presented in clause D.7.2 and can be expressed by Eq. (15).

$$X_d = \eta_d \frac{X_{k(n)}}{\gamma_m} = \frac{\eta_d}{\gamma_m} m_X \{1 - k_n V_X\},$$ (15)

where:

$X_{k(n)}$ is the characteristic value, including statistical uncertainty for a sample of size n with any conversion factor excluded,

η_d is the design value of the possible conversion factor (so far as it is not included in the partial factor for resistance γ_M),

γ_m is the partial factor that should be selected according to the field of application of the test results,

m_X is the mean of the n sample results,

k_n is the characteristic fractile factor,

V_X is the coefficient of variation of X, given by s_X / m_X with $s_X^2 = \dfrac{1}{n-1}\sum (x_i - m_X)^2$.

The factors η_d and γ_m were considered equal to one in the calculations presented, since they are included in the partial safety factor given by $\gamma_{M2} = 1.25$ (CEN 2004).

The methods for the determination of resistance models are presented in clause D.8, namely method (a) which is used in this paper. This method is divided into several steps, the first is the development of a theoretical resistance model (Eq. (16)).

$$r_t = g_{rt}(X).$$

(16)

This theoretical model should cover all the basic variables that can affect the resistance and all basic parameters should be available for use in the evaluation. In step two, the resistance values calculated by the previously developed theoretical model (r_{ti}) should be compared with the experimental ones (r_{ei}) resulting in the diagram of Fig. 7. It is possible to determine the mean value correction factor (Eq. (17)) from this diagram and, from this, it is possible to estimate the coefficient of variation of the error term δ (Eq. (21)).

$$b = \frac{\sum r_e r_t}{\sum r_t},$$

(17)

$$\Delta_i = \ln(\delta_i) = \ln\left[\frac{r_{ei}}{br_{ti}}\right],$$

(18)

$$\overline{\Delta} = \frac{1}{n}\sum_{i=1}^{n}\Delta_i,$$

(19)

$$s_\Delta^2 = \frac{1}{n-1}\sum_{i=1}^{n}(\Delta_i - \overline{\Delta})^2,$$

(20)

$$V_\delta = \sqrt{\exp(s_\Delta^2) - 1},$$

(21)

where:

b	is a correction factor,
r_e	is the experimental resistance value,
r_t	is the theoretical resistance determined from the resistance function $g_{rt}(X)$,
r_{ei}	is the experimental resistance for specimen i,
r_{ti}	is the theoretical resistance determined, using the measured parameters X for specimen i,
Δ	is the logarithm of the error term δ [$\Delta_i = ln(\delta_i)$],
$\overline{\Delta}$	is the estimated value for $E(\Delta)$,
s_Δ	is the estimated value of standard deviation,
V_δ	is the estimator for the coefficient of variation of the error term δ.

Since the present experimental study was composed by 42 experimental tests (less than 100), the last step takes the following form

$$r_k = bg_{rt}(X_m)\exp(-k_\infty\alpha_{rt}Q_{rt} - k_n\alpha_\delta Q_\delta - 0.5Q^2),$$

(22)

where
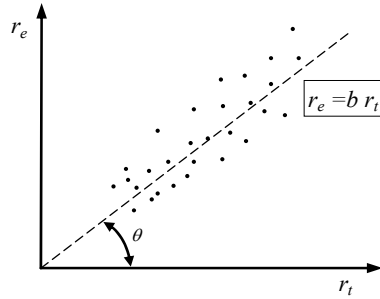
Fig. 7 Diagram r_e-r_t

$$V_{rt} = \sqrt{\sum_{i=1}^{j} V_{Xi}^2}, \tag{23}$$

$$Vr = \sqrt{V_\delta^2 + V_{rt}^2}, \tag{24}$$

$$Q_{rt} = \sqrt{\ln(V_{rt}^2 + 1)}, \tag{25}$$

$$Q_\delta = \sqrt{\ln(V_\delta^2 + 1)}, \tag{26}$$

$$Q = \sqrt{\ln(V_r^2 + 1)}, \tag{27}$$

$$\alpha_{rt} = \frac{Q_{rt}}{Q}, \tag{28}$$

$$\alpha_\delta = \frac{Q_\delta}{Q}, \tag{29}$$

k_∞ is the value of k_n for $n \rightarrow \infty$ [$k_\infty = 1.64$],
V_{Xi} is the coefficient of the variation of X_i.

3.3 Experimental programme

A set of simple specimens for shear tests to evaluate the behaviour of the alternative end anchorage mechanism and to gather results to calibrate an analytical model was prepared (see Table 1). The experimental programme consisted of testing 42 specimens divided into 3 types: A, B and C (see Fig. 8). Specimen types A and B have different distances from the rebar to the edge of the steel sheeting. This difference was intended to verify the influence of the edge distance on the bearing resistance. Specimen type C have 2 ribs which were intended to simulate the inner ribs of the slab where the rebar ends are inside the concrete, unlike the specimen types A and B that simulate an outer rib. In order to eliminate the friction shear force along the steel-concrete interface, the majority of the specimens (30 tests in accordance with Table 1) were prepared with flat steel sheeting with a mould release fluid along the interface. The remaining specimens were prepared with corrugated (with embossments) steel sheeting; in these specimens a 10 mm

Table 1 Overview of the experimental specimens

	Sheet	Sheet thickness (mm)	Rebar surface	Rebar diameter (mm)	Type	Number of specimens	Designation
1 rib	Flat	0.8	Smooth	φ10	A	3	FS1R - 01
				φ12	A	3	FS1R - 02
		1.0		φ10	A	3	FS1R - 03
				φ12	A	3	FS1R - 04
					B	3	FS1R - 05
			Ribbed	φ12	A	3	FR1R - 01
					B	3	FR1R - 02
	Embossments		Smooth	φ12	A	3	ES1R - 01
			Ribbed			3	ER1R - 01
2 ribs	Flat	1.0	Smooth	φ10	C	3	FS2R - 01
				φ12	C	3	FS2R - 02
			Ribbed	φ12	C	3	FR2R - 01
	Embossments		Smooth	φ12	C	3	ES2R - 01
			Ribbed		C	3	ER2R - 01

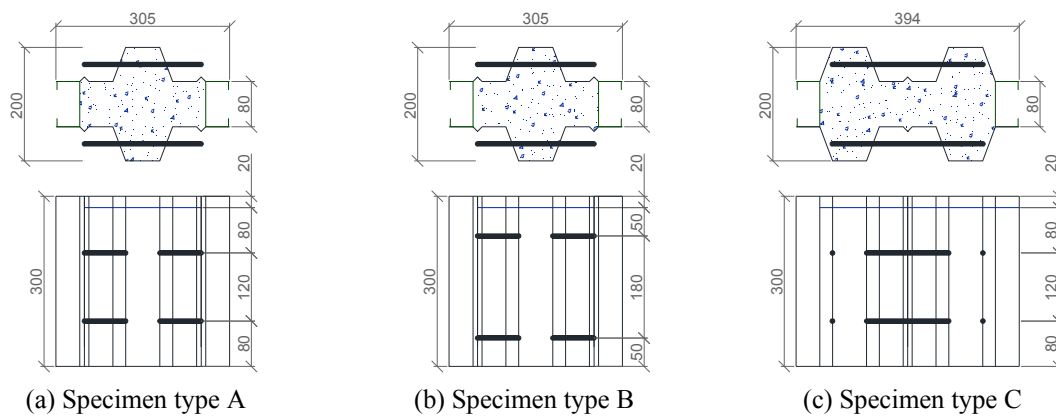(a) Specimen type A (b) Specimen type B (c) Specimen type C

Fig. 8 Specimen geometry

polystyrene sheet was introduced to prevent the interlock resistance between the embossments and the concrete (see Fig. 9(a)). Some specimens were fabricated with ribbed rebars to evaluate the influence of the roughness of rebars on the bearing resistance (see Table 1). The 20 mm gap between the concrete edge and the steel sheeting edge (shown in Fig. 8) was designed to allow the displacement of the sheet in relation to the rebars (joined to the concrete). On the opposite side of this gap, a 20 mm thick steel plate (Fig. 9(b)) was introduced in order to transmit the load to the concrete and measure it by four 10 tonne load cells. The rebar-steel sheet displacement was measured on two of the four rebars with displacement transducers of 25 mm capacity (Fig. 9(c)). All data was recorded by a data-logger system. The load was applied by a compression test machine with a constant displacement speed of 0.01 mm/s up to a displacement of 5 mm, followed

(a) Expanded polystyrene sheet application

(b) 20 mm thick steel plates and load cells with a 10 tonne capacity

(c) Displacement transducer to measure the relative displacement

Fig. 9 Details of specimens and measurement equipment

by a speed of 0.02 mm/s until the collapse.

The materials used in the manufacturing of the specimens were submitted to tests to characterize their mechanical properties, except the rebar steel because its resistance and stiffness was not involved in the failure modes of the specimens. Thereby, concrete cubes (150 mm of edge) were submitted to compression tests in accordance with EN 12390, part 3 (CEN 2002b) and the sheet steel specimens were submitted to uniaxial tension tests in accordance with ISO 6892-1, part 1 (ISO 2009). Mean values for the concrete compressive strength of 29.66 MPa in the first specimens (0.8 mm thick steel sheet) and 21.26 MPa in the second specimens (1.00 mm thick steel sheet) were obtained from these tests. The 0.8 mm thick steel sheet had a mean yield strength of 379.04 MPa and a mean ultimate strength of 419.28 MPa; for the 1.0 mm thick steel sheet, 262.9 MPa for the mean yield strength and 345.99 MPa for the mean ultimate strength were obtained.

Graphs of Figs. 10, 11 and 12 represent the mean load-displacement curves for each group of specimens. The graph displayed in Fig. 10 refers to specimens with flat sheet, smooth rebar and one rib; it is possible to conclude from this graph that, as expected, the increase in the sheet thickness (from FS1R - 01 to FSR - 03) or the rebar diameter (from FS1R - 02 to FSR - 04) results
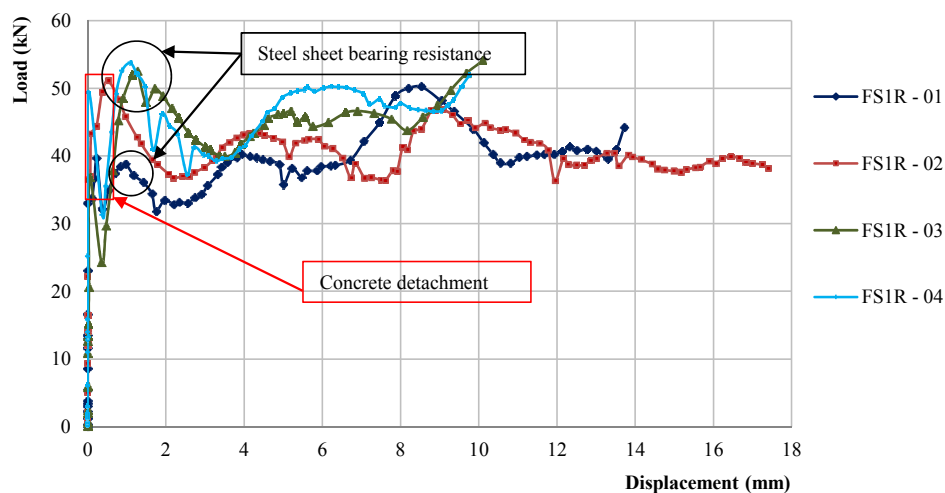

Fig. 10 Load-displacement curves for specimens with one rib, flat sheet and smooth rebars
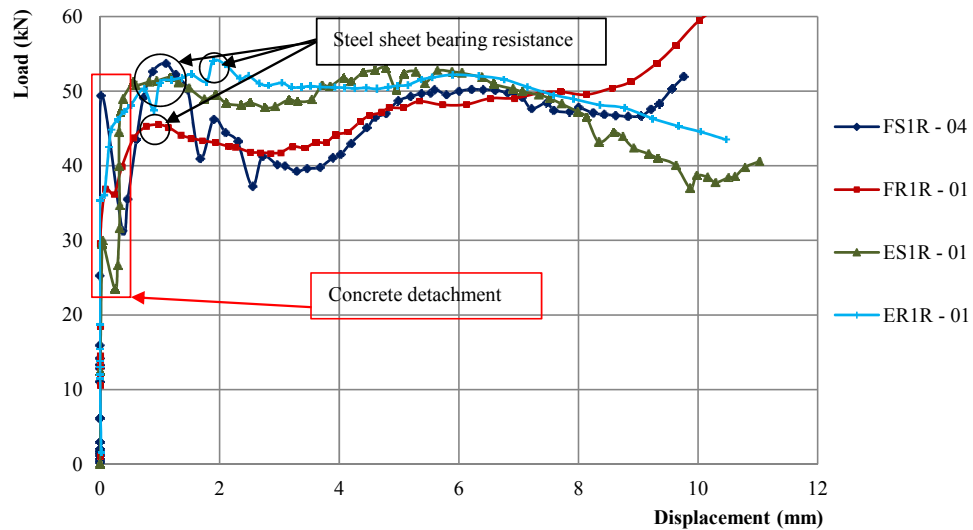
Fig. 11 Load-displacement curves for specimens with one rib, 1.0 mm thick flat sheets and sheets with embossments and smooth or ribbed 12 mm diameter rebars
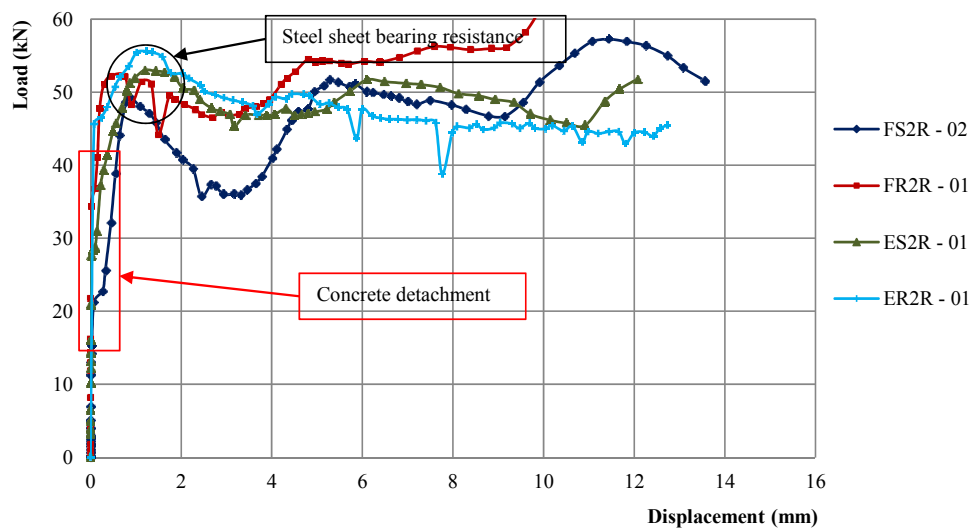

Fig. 12 Load-displacement curves for specimens with two ribs, 1.0 mm thick flat sheets and sheets with embossments and smooth or ribbed 12 mm diameter rebars

Fig. 13 Dismantled specimen

in an increase in the bearing resistance of the sheet and therefore in an increase in the end anchorage resistance. The load-displacement curves for the one rib specimens, flat sheets and sheets with embossments of 1.0 mm thickness and smooth or ribbed 12 mm diameter rebars (specimens FS1R - 04, FR1R - 01, ES1R - 01 and ER1R - 01) are represented in Fig. 11. It can be seen that similar results were obtained for the different combinations between flat sheets or sheets with embossments and smooth or ribbed rebars, after analysing the data. The exception was the combination of flat sheet with ribbed rebar (specimens FR1R - 01) for which a lower value was btained. However, this result may have been affected by some experimental error because the results for the equivalent combination, in the series of tests of specimens with two ribs (specimen FR2R - 01), were similar to the others (see Fig. 12). The graph in Fig. 12 presents the load-displacement curves for specimens with two ribs and the same combinations of sheet and rebars presented in the graph in Fig. 11. From this data, it is possible to validate the previous conclusion, which establishes that different combinations between flat sheet or sheet with embossments and smooth or ribbed rebar, lead to similar results.

The results from the tests with type B specimens (not presented in this paper) were similar to the ones presented for type A; therefore, it is possible to conclude that all the results are valid for rebars with an edge distance of, at least, 50 mm (Fonseca 2012).

After inspecting the specimens dismantled after the tests (see Fig. 13), it was possible to conclude that the concrete did not influence the resistance because the chemical bond between it and the steel sheet was broken before the maximum end anchorage resistance had been reached. In the following sections and in accordance with the previous analysis of the test results, it is considered that the bearing resistance is dependent on the sheet thickness and rebar diameter. The remaining parameters, such as the roughness of the rebar, sheet embossments or rebar position (inner or outer rib) are not considered as influential.

Table 2 Characteristic values of bearing resistance

Specimen group	x_i (kN)	n	m_X (kN)	s_X^2	V_X	k_n	η_d	γ_m	X_k (kN) Total (8 contact points)	X_k (kN) By contact point
FS1R - 01	41.99; 38.80; 39.63	3	40.14	2.73	0.10	3.37	1	1	26.61	3.33
FS1R - 02	46.83; 45.08; 45.37	3	45.76	0.88	0.10	3.37	1	1	30.34	3.79
FS1R - 03	-; -; 52.47	3	-	-	-	-	1	1	-	-
FS1R - 04	53.74; 55.99; 53.39	3	54.37	1.99	0.10	3.37	1	1	36.05	4.51
FS1R - 05	45.67; 45.48; 45.51	3	45.55	0.01	0.10	3.37	1	1	30.20	3.78
FR1R - 01	51.87; 53.87; 57.98	3	54.57	9.71	0.10	3.37	1	1	36.18	4.52
FR1R - 02	52.49; 54.06; 53.93	3	53.49	0.76	0.10	3.37	1	1	35.47	4.43
ES1R - 01	48.77; 48.98; 49.17	3	48.97	0.04	0.10	3.37	1	1	32.47	4.06
ER1R - 01	47.99; 50.89; 47.76	3	48.88	3.06	0.10	3.37	1	1	32.41	4.05
FS2R - 01	48.80; 55.30; 54.03	3	52.71	11.85	0.10	3.37	1	1	34.95	4.37
FS2R - 02	49.27; 52.82; 60.67	3	54.25	34.02	0.11	3.37	1	1	34.59	4.32
FR2R - 01	51.76; 52.23; 51.29	3	51.76	0.22	0.10	3.37	1	1	34.32	4.29
ES2R - 01	52.99; 62.53; 62.59	3	59.37	30.50	0.10	3.37	1	1	39.36	4.92
ER2R - 01	63.89; 55.57; 56.02	3	58.49	21.91	0.10	3.37	1	1	38.78	4.85

Alexandre Fonseca, Bruno Marques and Rui Simões

3.4 Statistical analysis of results

The experimental results were analysed according to Eq. (15) to determine the characteristic value of the bearing resistance (end anchorage resistance). Since 3 specimens were tested for each combination of steel sheet and rebar, the factor k_n takes the value of 3.37, in accordance with Table D1 of EN 1990 (CEN 2002a). Table 2 presents the statistical analysis of the results from the various groups of 3 specimens (described in Table 1); the experimental bearing resistance x_i was established as the maximum load reached after concrete detachment.

In accordance with the procedure described in Annex D of EN 1990 (CEN 2002a), the Eq. (14) was used as the theoretical resistance model. Table 3 displays the theoretical characteristic values for the resistance, calculated with the real material properties for the various sheet thickness and rebar diameter combinations. Based on the experimental and theoretical results, the diagram $F_{b,ke}$-$F_{b,kt}$ shown in Fig. 14 was defined and the factor $b = 0.7077$ was determined from Eq. (17). In the base model, the only variable is the ultimate strength of the steel sheet, thus it was necessary to determine its variation coefficient – V_{Xi} (see Table 4). The coefficient calculated was compared with other papers published on the topic (Karmazínová and Melcher 2011, Rebelo *et al*. 2008, Simões da Silva *et al*. 2008, Wiśniewski *et al*. 2012) using the value $V_{Xi} = 0.05$. Solving the equations presented above (Eqs. (23)-(29)) and using their values in Eq. (22) we reach the resistance model (Eq. (31)).

Table 3 Theoretical characteristic resistance $F_{b,kt}$

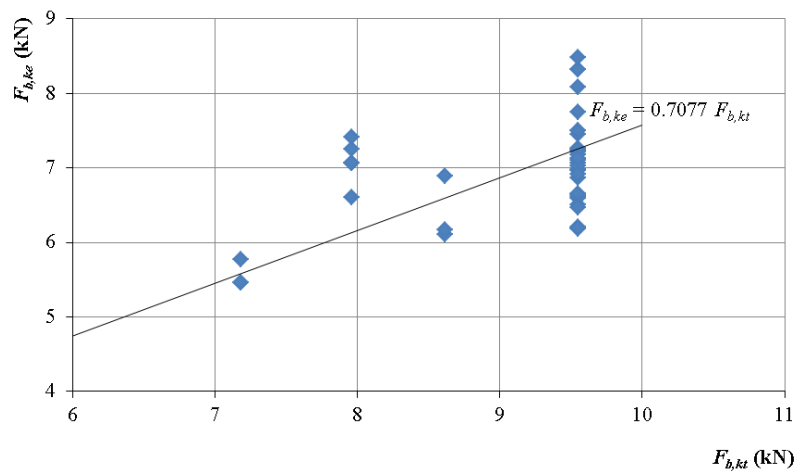| Sheet thickness (mm)	Rebar diameter (mm)	e_1 (mm)	f_u (MPa)	α_b	k_t	γ_{M2}	$F_{b,kt}$ (kN)
0.8	10	80	419.28	1	0.856		7.18
	12						8.61
1	10	80	345.99	1	0.92	1	7.96
	12						9.55
1	12	50	345.99	1	0.92		9.55

Fig. 14 Diagram $F_{b,ke}$ - $F_{b,kt}$

Table 4 Determination of the ultimate strength variation coefficient of the steel sheet

Sheet thickness	Specimen	Ultimate strength $f_{u,i}$ (MPa)	Mean value ultimate strength f_{upm} (MPa)	Standard deviation	Variation coefficient V_{Xi}
0.8 mm	P1	415.51	419.28	11.540	0.028
	P2	420.22			
	P3	422.10			
1.0 mm	P4	350.59	345.99	17.352	0.050
	P5	344.92			
	P6	342.47			

$$F_{b,k} = 0.7077\, F_{b,kt}\, \exp(-1.64 \times 0.4395 \times 0.05 - 1.73 \times 0.8994 \times 0.1023 - 0.5 \times 0.1137^{2}), \quad (30)$$

$$F_{b,k} = 0.5784\, F_{b,kt} \Leftrightarrow F_{b,d} = 0.5784\, F_{b,Rd} = 0.5784 \frac{2.5\, \alpha_b\, k_t\, f_u\, d\, t}{\gamma_{M2}}. \quad (31)$$

The calibration of the model could be improved more if larger data sets were used. Therefore, further tests with specimens of different materials and geometrical properties will be necessary.

4. Composite slabs with transversal rebars as end anchorage

4.1 Introduction

An experimental programme was carried out to study the effect of the proposed alternative end anchorage mechanism on the behaviour of simple supported composite slabs in part 2 of the present study. The experimental results were compared with the analytical results predicted through the partial connection method of Eurocode 4 (CEN 2007). The analytical prediction of the slab resistance is a review of the previous results published (Marques and Simões 2011) but now the calibrated model for predicting the resistance of the alternative end anchorage mechanism developed in the scope of the present paper will be used.

4.2 Characterization of the materials

The steel sheeting used in the tests was composed by a profile H-60 with a thickness of 1 mm and height of 60 mm, manufactured by a Portuguese steel company; the steel, grade S320 GD+Z in accordance with EN 10346 (CEN 2009), presented a mean value of the yield strength given by $f_{yp,m}$ = 321.9 MPa. The rebars, with a diameter of 12 mm and f_{sk} = 500 MPa (nominal value), presented a mean value of the tensile strength f_{sm} = 578.4 MPa. The concrete presented a mean value of the cylinder compressive strength f_{cm} = 31.4 MPa.

4.3 Description of the experimental models

The experimental programme consisted of the realization of 8 experimental tests, divided in four groups (two similar models in each group), as described in Table 5. The models A11 and A12

Table 5 Slab models

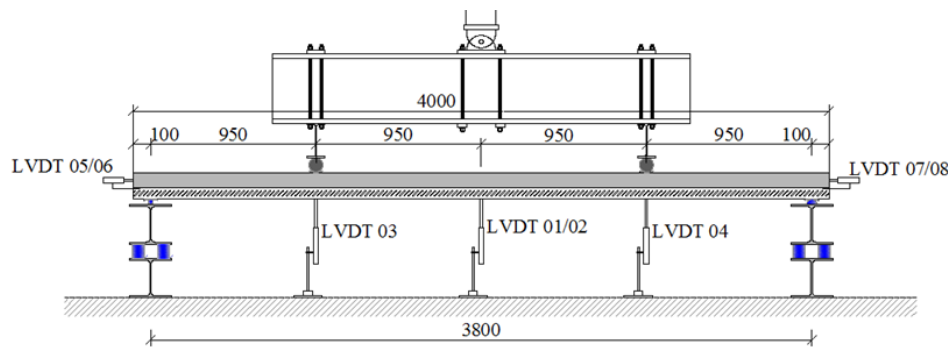| Slab model	Model description	Weight (kg)
A11; A12	Slab without any reinforcement	891; 953
A21; A22	Slab with one transversal rebar at each extremity	1018; 957
A31; A32	Slab with one longitudinal rebar on each rib	946; 966
A41; A42	Slab with one longitudinal rebar on each rib and one transversal rebar on each extremity	993; 956

Fig. 15 Test set-up and instrumentation

were the base models, used to compare with the remaining improved models. The improved models consisted of slabs with transversal rebars close to the supports (models A21 and A22), slabs with longitudinal rebars on the ribs (models A31 and A32) or slabs with rebars in both directions (models A41 and A42). The composite slab models had a width of 820 mm, a total height of 150 mm and a total length of 4000 mm with 3800 mm between supports (see Fig. 15).

The experimental tests were carried out in accordance with the procedures prescribed in Annex B of EN 1994-1-1 (CEN 2007). In the models, strain gauges were applied on the steel sheeting and rebars, load cells were placed on the supports to measure the reactions, as well as several linear displacement transducers (LVDTs) to measure vertical displacements along the span and horizontal slip displacements between the steel and concrete at the extremities (Fig. 15).

4.4 Analysis of experimental results

The tests were carried out by applying an increased load (two loads at 1/4 of span) until failure, with a controlled displacement increment of 0.012 mm/s. Fig. 16 shows the experimental test set-up.

Tests A11 and A12 presented the behaviour expected. The collapse was governed by the longitudinal shear failure and the maximum load was attained after the occurrence of end slips. In the subsequent tests (A21 and A22), the transversal rebar induced an end anchorage effect. So, the maximum load was increased and the end slip was insignificant. The collapse mode was the bearing of the steel sheeting, as shown in Fig. 17 in this group. The effect of end anchorage due to the two transversal rebars (one at each extremity) was an increase of initial stiffness, maximum attained load and ductility. In terms of resistance, the mean value of the maximum load attained in the two first tests (A11 and A12) was 38.85 kN, while in the second two tests (A21 and A22 with
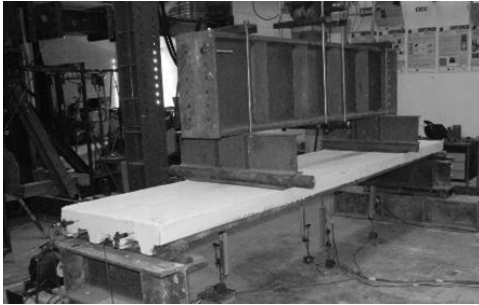
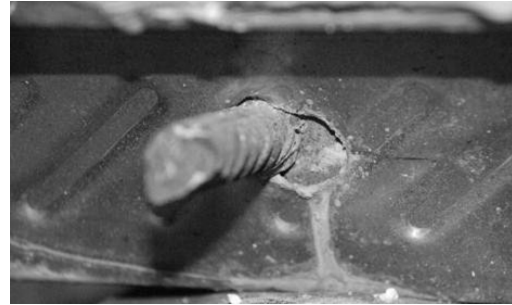Fig. 16 Experimental test set-up

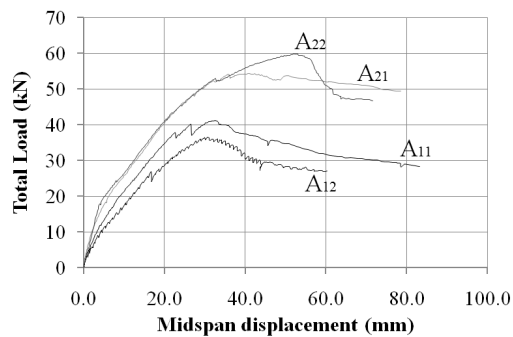Fig. 17 Bearing of the steel sheeting
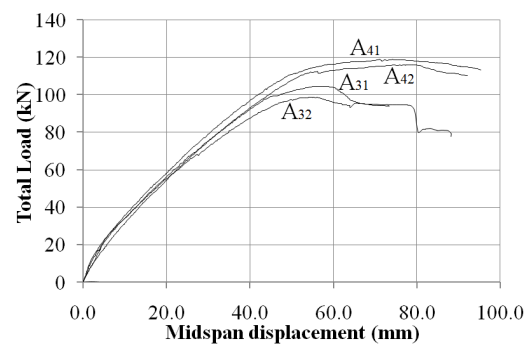

Fig. 18 Load-displacement curves (A11 to A22)

Fig. 19 Load-displacement curves (A31 to A42)

two reinforcement rebars) the equivalent value was 57.01 kN, 46.7% higher. The curves relating the total load with the vertical displacement at mid-span of the slabs of this group are represented in Fig. 18.

In practice, sometimes a rebar is placed along the ribs to increase the slab resistance and stiffness and to improve fire performance. So, to evaluate the effect of the end anchorage assured by one transversal rebar at each extremity, a second group of tests, as indicated in Table 5 (A31, A32, A41 and A42) was carried out. For this group, the load-vertical displacement curves are shown in Fig. 19. In this case, the initial stiffness was similar in all the slabs tested, but in the slab models with transversal reinforcement (A41 and A42) the mean value of the maximum load attained was 15.4% higher and the ductility was also increased.

4.5 Prediction of the resistance of slabs A11, A12, A21 and A22

In order to determine the expected slab resistance of the slab models A11, A12, A21 and A22, the partial connection method (described in Section 2.1 above) was used together with the end anchorage resistant model, described and calibrated in the scope of the present paper (Section 3). The longitudinal shear strength given by $\tau_{u,Rd} = 0.185$ MPa was determined previously to apply the partial connection method (Marques and Simões 2011). Figs. 20 and 21 summarize all the calculations carried out, showing the diagram of the resistant bending moment predicted on half of the slab. From Fig. 20 it can be noted that the maximum acting bending moment in slabs without transversal reinforcement, $M_{test} = 21.62$ kNm (a mean value of test results), is only 57% of the
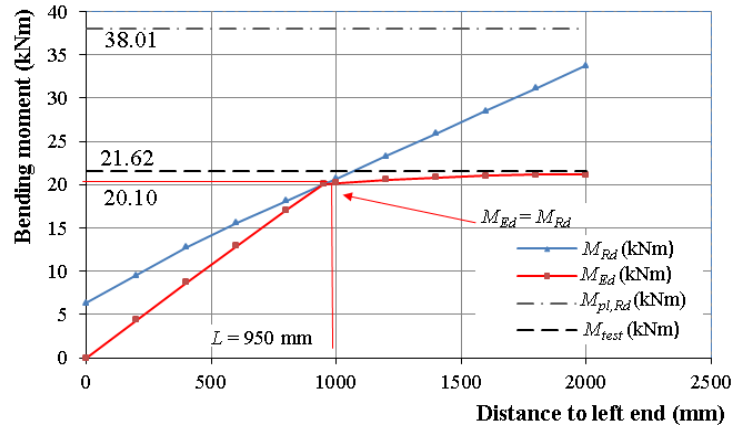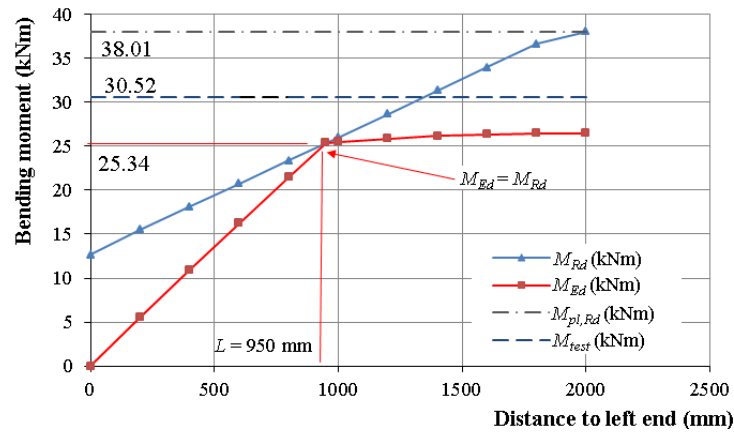
Fig. 20 Bending moment in slabs A11 and A12

Fig. 21 Bending moment in slabs A21 and A22

predicted plastic bending resistance $M_{pl,Rd}$ of the composite slab in full shear connection. The maximum acting bending moment in the slabs with one transversal rebar at each extremity, $M_{test} = 30.52$ kNm (a mean value of test results), increased to about 80% of the predicted plastic resistance $M_{pl,Rd}$ of the composite slab in full shear connection (see Fig. 21).

In slabs without transversal reinforcement, the expected maximum bending moment (the characteristic value) is 20.10 kNm and the experimental maximum bending moment (M_{test}) was 21.62 kNm, 7.6% higher. In slabs with transversal reinforcement, the expected maximum bending moment (the characteristic value) is 25.34 kNm and the experimental maximum bending moment (M_{test}) was 30.52 kNm, 20.4% higher.

4.6 Prediction of the resistance of slabs A31, A32, A41 and A42

The resistance of the slab models A31, A32, A41 and A42 can be predicted through the formulation described in Section 2.2 above. It can be seen in Fig. 22 that the maximum acting bending moment in slabs without transversal reinforcement, $M_{test} = 51.54$ kNm (a mean value of
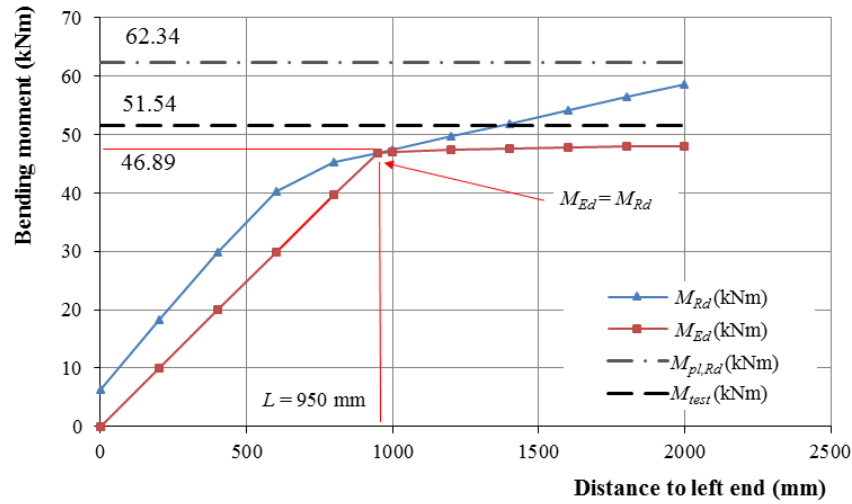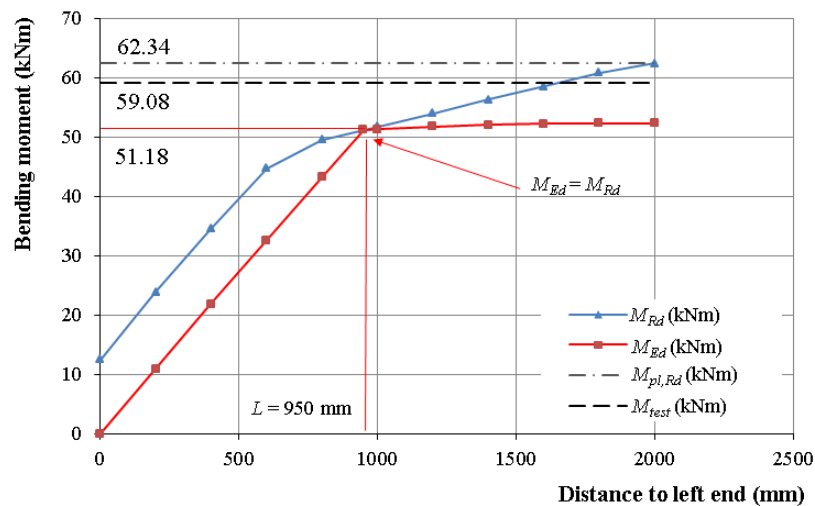
Fig. 22 Bending moment in slabs A31 and A32

Fig. 23 Bending moment in slabs A41 and A42

test results), is 83% of the predicted plastic bending resistance $M_{pl,Rd}$ of the composite slab in full shear connection. In the slabs with one transversal rebar at each extremity (see Fig. 23), the maximum acting bending moment in slabs, M_{test} = 59.08 kNm (a mean value of test results), increased to about 95% of the predicted plastic resistance $M_{pl,Rd}$ of the composite slab in full shear connection.

In slabs A31 and A32 the predicted bending moment (characteristic value) was 46.89 kNm and the average bending moment attained in experimental tests (M_{test}) was 51.54 kNm, which corresponds to a 9.9% higher value (Fig. 22).

In slabs A41 and A42 the predicted bending moment (characteristic value) was 51.18 kNm and the average bending moment attained in the experimental tests (M_{test}) was 59.08 kNm, 13.4% higher.

5. Conclusions

In Section 3, the determination of the resistance of an alternative end anchorage mechanism with transversal rebars crossing steel sheeting was described, based on an experimental programme and posterior statistical analysis of the results in accordance with Annex D of EN 1990 (CEN 2002a). From this part of the work, we may conclude that:

- as predictable, the end anchorage resistance increases with the increase in the thickness of the steel sheet and the increase in the diameter of the rebar;
- the resistance of the end anchorage was governed by the bearing resistance of the steel sheet, thus, the greater the resistance or thickness of the steel sheet is, the more effective it is;
- the anchorage resistance is independent of whether the rebar extremities are inside (inner rib as reproduced in specimens type C) or outside (outer rib as reproduced in specimens type A or B) the concrete;
- the replacement of embossed steel sheeting by a flat one (without embossments), in general, leads to similar results;
- the results determined are valid for an end distance of at least 50 mm; for lower distances the extremity effect should be taken into account by means of the α_b factor.

In Section 4 a second experimental programme was presented which intended to study the influence of the alternative end anchorage mechanism proposed on the behaviour of simple supported composite slabs. Additionally, the influence of using longitudinal rebars on the ribs was also addressed. The following conclusions were reached from this part of the programme:

- the results obtained proved that slab capacity and slab ductility may be increased with the proposed alternative end anchorage mechanism; in the tests carried out, the plastic bending moment of the composite slabs, in the case of full shear connection, was not reached with one rebar on each side, but could be, by increasing the number of transversal rebars or the thickness of steel sheeting;
- the additional difficulty, in terms of sheet production and erection on site, is certainly the main disadvantage of the end anchorage mechanism proposed; this issue is still being analysed, with the cooperation of some Portuguese steel companies;
- from the present study, it may also be concluded that the partial connection method of Eurocode 4 (CEN 2007), if reformulated to incorporate the proposed end anchorage mechanism and/or longitudinal rebars on ribs, may be used to predict the slab resistance with adequate accuracy;
- the maximum differences, between the predicted characteristic resistance and the experimental resistance, of 20.4% in slab models A21 and A22 and 13.4% in slab models A41 and A42 may be due to an increase of the slip force between the steel sheeting and the concrete in the area around the transversal rebars close to the supports. This effect was not fully reproduced in the tests carried out to calibrate the end anchorage resistance model (described in Section 3) because these tests did not include a normal force, which is always present in a real slab. This lacuna can be filled by suitable additional tests.

References

Carmona, R.L., Branco, J.C. e Simões, R. (2009), "Lajes mistas com chapa colaborante: Soluções para melhorar o seu comportamento", *VII Congresso de Construção Metálica e Mista* pag. II-593 a II-604,

Lisboa, Portugal. [In Portuguese]

CEN (1992), prENV 1994-1-1 – Eurocode 4 - Design of composite steel and concrete structures - Part 1-1: General rules and rules for buildings, European Committee for Standardization, Brussels, Belgium.

CEN (2002a), EN 1990 – Eurocode 0 – Basis of structural design, European Committee for Standardization, Brussels, Belgium.

CEN (2002b), EN 12390 – Testing hardened concrete, Part 3: Compressive strength of test specimens, European Committee for Standardization, Brussels, Belgium.

CEN (2004), EN 1993-1-3 – Eurocode 3 – Design of steel structures – Part 1-3: General rules – Supplementary rules for cold-formed members and sheeting, European Committee for Standardization, Brussels, Belgium.

CEN (2007), EN 1994-1-1 – Eurocode 4 - Design of composite steel and concrete structures - Part 1-1: General rules and rules for buildings, European Committee for Standardization, Brussels, Belgium.

CEN (2009), EN 10346 – Continuously hot-dip coated steel flat products - Technical delivery conditions, European Committee for Standardization, Brussels, Belgium.

CEN (2010), EN 1993-1-8 – Eurocode 3 – Design of steel structures – Part 1-8: Design of joints, European Committee for Standardization, Brussels, Belgium.

Chen, S. (2003), "Load carrying capacity of composite slabs with various end constrains", *J. Construct. Steel Res.*, **59**(3), 385-403.

Chen, S., Shi, X. and Qiu, Z. (2011), "Shear bond failure in composite slabs – A detailed experimental study", *Steel Compos. Struct.*, *Int. J.*, **11**(3), 233-250.

Chuan, D.L., Abdullah, R. and Bakar, K.B. (2008), "Behaviour and Load Bearing Capacity of Composite Slab Enhanced with Shear Screws", *Malay. J. Civil Eng.*, **20**(2), 284-294.

Ferrer, M., Marimon, F., Roure, F. and Crisinel, M. (2005), "Optimised design of a new profiled steel sheet for composite slabs using 3d non-linear finite elements", *Proceedings of the 4th Eurosteel Conference on Steel and Composite Structures*, Maastricht, Netherlands, June.

Fonseca, A. (2012), "Calibração Experimental de um Modelo Analítico de Cálculo de Sistemas de Amarração de Extremidade em Lajes Mistas", Dissertação apresentada para obtenção do grau de Mestre em Engenharia Civil na Especialidade de Mecânica Estrutural, DEC-FCTUC, Coimbra, Portugal. [In Portuguese]

ISO 6892-1 (2009), Metallic materials - Tensile testing. Part 1: Method of test at room temperature, International Organization for Standardization, Switzerland.

Johnson, R.P. (2004), *Composite Structures of Steel and Concrete* (*Volume 1*): *Beams*, *Columns*, *Frames and Applications in Buildings*, (3rd Edition), Blackwell, Oxford, UK.

Johnson, R.P. and Anderson, D. (2004), Designer's Guide to EN 1994-1-1 – Eurocode 4: Design of composite steel and concrete structures, Part 1.1: General rules and rules for buildings, Thomas Telford, London, UK.

Jolly, C.K. and Lawson, R.M. (1992), "End anchorage in composite slabs: an increased load-carrying capacity", *The Structural Engineer*, **70**(11), 202-205.

Karmazínová, M. and Melcher, J. (2011), "Design assisted by testing applied to the determination of the design resistance of steel-concrete composite columns", *Mathematical Methods and Techniques in Engineering and Environmental Science*, Catania, Italy, pp. 420-426. ISBN 978-1-61804-046-6

Lopes, E. and Simões, R. (2008), "Experimental and analytical behaviour of composite slabs", *Steel Compos. Struct.*, *Int. J.*, **8**(5), 361-388.

Marques, B. and Simões, R. (2011), "Improvement of the behavior of composite slabs", (L. Dunai, M. Ivanyi, K. Jarmai, N. Kovacs and L. Gerleny Vigh Eds.), *EuroSteel 2008 – 5th European Conference on Steel and Composite Structures – Research – Design – Construction*, *ECCS*, Budapest, Hungary, pp. 639-644.

Rebelo, C., Lopes, L., Simões da Silva, L., Nethercot, D. and Vila real, P.M.M. (2008), "Statistical evaluation of the lateral-torsional buckling resistance of steel I-beams, Part 1: Variability of the Eurocode 3 Resistance model", *J. Construct. Steel Res.*, **65**(4), 818-831.

Simões da Silva, L., Rebelo, L., Nethercot, D., Marques, L., Simões, R. and Vila real, P.M.M. (2008),

"Statistical evaluation of the lateral-torsional buckling resistance of steel I-beams, Part 2: Variability of steel properties", *J. Construct. Steel Res.*, **65**(4), 832-849.
Wiśniewski, D.F., Cruz, P.J.S., Henriques, A.A.R. and Simões, R. (2012), "Probabilistic models for mechanical properties of concrete reinforcing steel and prestressing steel", *Struct. Infrastruct. Eng. Maint. Manag., Life-Cycle Des. Perform.*, **8**(2), 111-123.

DL